

Faster Video Moment Retrieval with Point-Level Supervision

Xun Jiang

University of Electronic Science and
Technology of China
Chengdu, China

Zailei Zhou

University of Electronic Science and
Technology of China
Chengdu, China

Xing Xu

University of Electronic Science and
Technology of China
Chengdu, China

Yang Yang

University of Electronic Science and
Technology of China
Chengdu, China

Guoqing Wang

University of Electronic Science and
Technology of China
Chengdu, China

Heng Tao Shen

University of Electronic Science and
Technology of China
Chengdu, China
Peng Cheng Laboratory
Shenzhen, China

ABSTRACT

Video Moment Retrieval (VMR) aims at retrieving the most relevant events from an untrimmed video with natural language queries. Existing VMR methods suffer from two defects: (1) massive expensive temporal annotations are required to obtain satisfying performance; (2) complicated cross-modal interaction modules are deployed, which lead to high computational cost and low efficiency for the retrieval process. To address these issues, we propose a novel method termed Cheaper and Faster Moment Retrieval (CFMR), which well balances the retrieval accuracy, efficiency, and annotation cost for VMR. Specifically, our proposed CFMR method learns from point-level supervision where each annotation is a single frame randomly located within the target moment. It is $6 \times$ cheaper than the conventional annotations of event boundaries. Furthermore, we also design a concept-based multimodal alignment mechanism to bypass the usage of cross-modal interaction modules during the inference process, remarkably improving retrieval efficiency. The experimental results on three widely used VMR benchmarks demonstrate the proposed CFMR method establishes new state-of-the-art with point-level supervision. Moreover, it significantly accelerates the retrieval speed with more than $100 \times$ FLOPs compared to existing approaches with point-level supervision.

CCS CONCEPTS

• **Computing methodologies** → **Activity recognition and understanding**; • **Information systems** → *Multimedia information systems*.

KEYWORDS

Video Moment Retrieval; Point-level Supervised Learning; Model Efficiency; Video Understanding; Multimedia Embedding

Permission to make digital or hard copies of all or part of this work for personal or classroom use is granted without fee provided that copies are not made or distributed for profit or commercial advantage and that copies bear this notice and the full citation on the first page. Copyrights for components of this work owned by others than ACM must be honored. Abstracting with credit is permitted. To copy otherwise, or republish, to post on servers or to redistribute to lists, requires prior specific permission and/or a fee. Request permissions from permissions@acm.org.
Conference'17, July 2017, Washington, DC, USA

© 2023 Association for Computing Machinery.
ACM ISBN 978-x-xxxx-xxxx-x/YY/MM...\$15.00
<https://doi.org/10.1145/nnnnnnn.nnnnnnn>

ACM Reference Format:

Xun Jiang, Zailei Zhou, Xing Xu, Yang Yang, Guoqing Wang, and Heng Tao Shen. 2023. Faster Video Moment Retrieval with Point-Level Supervision. In *Proceedings of ACM Conference (Conference'17)*. ACM, New York, NY, USA, 10 pages. <https://doi.org/10.1145/nnnnnnn.nnnnnnn>

1 INTRODUCTION

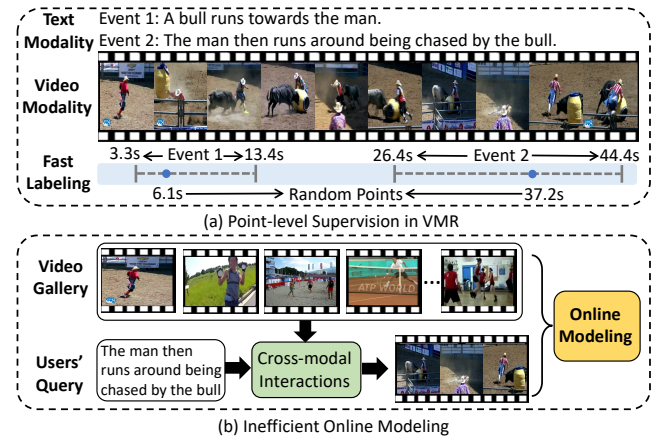


Figure 1: An illustrative example of PS-VMR and a problem in applications: (a) The annotated points are located within the target moment randomly, which can be labeled much faster and cheaper according to [21]. (b) Existing methods have to conduct cross-modal interactions among videos and text queries online, which limits model efficiency heavily.

Video Moment Retrieval (VMR) aims at retrieving the startings and endings of particular events in an untrimmed video, with given natural language queries. It was first proposed in [1, 9] and gradually formed two types in terms of the training data annotations: Fully-Supervised VMR (FS-VMR) [1, 8–10, 25, 33, 37] and Weakly-Supervised VMR (WS-VMR) [5, 18, 23, 38, 39]. The former, which is the earliest VMR paradigm, contains the conventional VMR methods trained with fully annotated data, where the event boundaries in each video are labeled by annotators deliberately. However, it is expensive or even not available to gather clear and determined annotations in most applications, which limits the deployment of

these FS-VMR methods. To tackle this problem, recently researchers proposed the WS-VMR paradigm trained with video-text matching pairs only, thus significantly reducing the annotation cost. Unfortunately, as arbitrarily abandoning the temporal supervision signals, the WS-VMR methods obtain much worse performance and generalization compared with the conventional FS-VMR methods, especially on long videos.

To narrow the gap between accuracy and annotation cost, a novel solution for VMR is proposed, *i.e.*, *Point-level Supervised VMR (PS-VMR)* [6, 35]. As shown in Fig. 1(a), instead of labeling determined boundaries, the point-level supervision is built on the single frame only, which is randomly located within the target event. Compared with fully-supervised labels, point-level labels are much easier to be annotated. According to [16, 21], point-level supervision is $6 \times$ cheaper than traditional ones (the 50s vs. 300s per 1-min video) while labeling the actions or events in an untrimmed video. However, all three solutions of VMR employ complicated cross-modal interaction modules to align text and video modalities. It limits the retrieval process with low efficiency because of the *online modeling*, which can not conduct multimodal learning until receiving users' queries. As is depicted in Fig. 1(b), existing methods have to repeatedly process the videos with unpredictable queries thus wasting massive computational resources. A recent work [10] also pointed out this defect and proposed a fast VMR approach to improve retrieval efficiency via a knowledge distillation mechanism. Nevertheless, it is highly reliant on expensive annotated data, which still limits the deployment heavily. To this end, we are dedicated to exploring a more practical solution for VMR by achieving *balanced performance on accuracy, efficiency, and annotation cost*.

In this paper, we propose a simple but efficient PS-VMR model, termed *Cheaper and Faster Moment Retrieval (CFMR)*, which achieves competitive retrieval performance while significantly reducing annotation cost and computational consumption. Specifically, as is depicted in Fig. 2, it consists of three Transformer-based components: (1) Video Concept Encoder (VCE), (2) Text Concept Encoder (TCE), and (3) Semantic Reconstructor (SR). The VCE and TCE modules are designed to encode videos and text queries into a group of concept vectors that represent diverse semantics. Furthermore, the SR module is deployed to mine semantic cues for learning concepts of each modality during training. In the test stage, we disable the SR module and simply calculate cosine similarity among video and text concepts to retrieve related moments. It bypasses online cross-modal interactions thus significantly improving the efficiency and saving massive computational resources. We conduct extensive experiments on three widely used VMR benchmarks, *i.e.*, Charades-STA, ActivityNet-Captions, and TACoS. The experimental results demonstrate our CFMR method outperforms recent state-of-the-art PS-VMR methods and shows superior comprehensive performance.

To sum up, our primary contributions are as follows:

- We propose a novel Cheaper and Faster Moment Retrieval method that tackles the PS-VMR problem. It is simple but efficient and achieves a fair trade-off among the accuracy, efficiency, annotation cost for VMR.
- We deploy a Point-guided Contrastive Learning module in our model, which effectively utilizes point-level supervision

to guide the model to discriminate the semantics hidden in video and text modalities.

- We design a Concept-based Multimodal Alignment module that avoids online cross-modal interactions widely used in previous methods. It allows higher efficiency and saves massive computational resources.

2 RELATED WORKS

Fully-Supervised Video Moment Retrieval. The FS-VMR is the earliest VMR paradigm that proposed by [1, 9] and have been studied for several years. All the data in FS-VMR is fully annotated, where the starting and ending is available for each training instance. Typically, Zhang *et al.* [37] exploited a two-dimensional temporal adjacent networks to refine the proposal features, then furtherly calculate the correspondence between each moment and text query. Wang *et al.* [33] designed a dynamic convolution mechanism that fully leveraged the information in the text query to reduce the noise in the video modality. Moreover, Mun *et al.* [25] adopted proposal-free framework that need not generate candidates to achieve higher efficiency. Gao *et al.* [10] adopted a knowledge distillation mechanism to reduce the computational consumption in cross-modal interactions. Although the FS-VMR methods have achieved remarkable performance, they require massive temporal annotations, which greatly limit their deployment.

Weakly-Supervised Video Moment Retrieval. The WS-VMR paradigm aims at reducing the heavy annotation cost in the traditional FS-VMR paradigm and attracts many researchers' attention recently. It requires the VMR model to learn from fewer temporal annotations [12, 20] or only the matching information among text queries and videos [18, 23, 38, 39], or even be trained in a zero-shot manner without any extra supervision [11, 19, 26]. In general, most weakly-supervised learning methods follow [23], which are trained with the matching video-query pairs. For example, Lin *et al.* [18] designed a semantic completion module that predicted the masked important words according to the given visual context for semantic similarity estimation. Following [18], Zheng *et al.* [38, 39] introduced multiple Gaussian functions into WS-VMR to exploit both positive and negative proposals from the same video. However, because of canceling the temporal supervision roughly, the WS-VMR methods perform much worse compared with most FS-VMR methods, especially on long untrimmed videos.

Point-level Supervised Learning. Point-level Supervised Learning is a weakly-supervised learning paradigm and widely adopted to reduce the annotation cost. It turns complex and expensive annotations into rough but extremely simple annotations. For example, Bearman *et al.* [3] introduced the point-level supervision by annotating a single pixel for each instance in the semantic segmentation task. It is also widely adopted on point-level supervised object detection [15, 34]. As for video understanding tasks, single-frame supervision is deployed in several recent works [22, 24] to achieve competitive performance on localizing action in untrimmed videos. Following that, a group of point-level supervised works [16, 21] on untrimmed videos have been proposed and proves the labeling cost can be reduced 6 times with the point-level annotations. Recently, Cui *et al.* [6] and Xu *et al.* [35] introduced the point-level

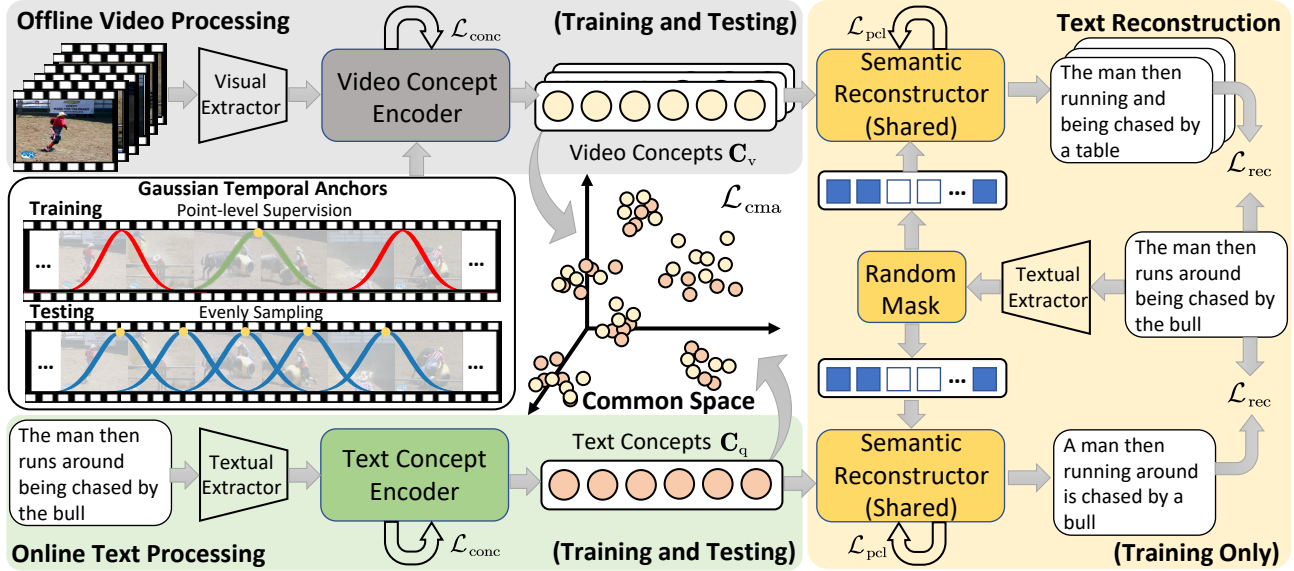


Figure 2: Illustration of our proposed CFMR method. The Video Concept Encoder and Text Concept Encoder learn concept representations for the two modalities respectively and project them into a common space to calculate cosine similarity. We also propose the Gaussian temporal anchors, where point-level supervision is adopted during training. The Semantic Reconstructor aims to explore the hidden semantics via masked query reconstruction, which is only enabled during training.

supervision signals into VMR, which reduce the heavy annotation cost while achieves competitive retrieval accuracy.

3 PROPOSAL METHOD

3.1 Problem Definition

We represent the training untrimmed video set as V , while the training text query set is represented as Q . For each test case, the input can be represented a untrimmed video v and a sentence query q . Let t_s and t_e be the start time and end time of one target video segment respectively, the VMR task can be formulated as $M_\theta(v, q; V, Q, A) \rightarrow \{(t_s, t_e)_k\}_{k=1}^K, t_s^k < t_e^k$. $(t_s, t_e)_k$ is the k -th retrieved moment in the ranked list of candidates. K is the number of predicted candidates, which is set to 1 in most proposal-free methods. The supervision signals are represented as A , which are definite temporal annotations or text-video pairs in FS-VMR and WS-VMR. However, in PS-VMR, the supervision signals are rough temporal points randomly located within target events rather than fully annotated labels.

3.2 Feature Extraction

Following the previous methods [6, 33, 39], we extract the video and text features in an offline manner. Firstly, given an untrimmed video V , we adopt the pre-trained visual backbones [4, 31] to extract the visual features. Moreover, we employ the GloVe [27] to extract the word-level embeddings of each sentence query Q . Let $M_v(\cdot), M_q(\cdot)$ be the pre-trained feature extractors of video and text modality respectively, the feature extraction is expressed as follows:

$$F_v = M_v(V) = \{f_v^i\}_{i=1}^{l_v}, F_q = M_q(Q) = \{f_q^j\}_{j=1}^{l_q}, \quad (1)$$

where the $F_v \in \mathbb{R}^{l_v \times d_v}$ and $F_q \in \mathbb{R}^{l_q \times d_q}$ represent the extracted video and text features respectively. d_v and d_q are feature dimensions for video and text modalities respectively. l_v and l_q are the total lengths of video features and number of words in the query.

3.3 Text/Video Concept Encoder

As is shown in Fig. 2, we adopt two Transformer-based components, *i.e.*, Text Context Encoder (TCE) and Video Context Encoder (VCE), to conduct intra-modality modeling respectively. Hence, there are no cross-modal interactions but projecting the two modalities into concept vector sequences with the same lengths.

Text Modality Encoding. Motivated by the success of BERT [7], we employ stacked multiple transformer encoders to learn the global representations for text modality progressively. Specifically, given the word-level features, we pad a $\langle CLS \rangle$ token at the end of the feature sequence, denoted as $F'_q = \{f_q^j, f_q^{cls}\}_{j=1}^{l_q}$. Let Φ_q be the text transformer encoders, this procedure can be formulated as:

$$H_q^{l+1} = \Phi_q(f_q(H_q^l)), H_q^1 = F'_q, \quad (2)$$

where $H_q^l \in \mathbb{R}^{(l_q+1) \times d_h}$ is encoded text feature sequence at l -th encoder layer. $f_q(\cdot)$ is the linear projection layer. d_h is the hidden feature dimension.

Video Modality Encoding. As most videos in the VMR task are untrimmed and contain multiple events and massive irrelevant content, we regard the potential event moments as foregrounds in long untrimmed videos. Inspired by the object detection [28, 30], we design the Gaussian temporal anchor mechanism to generate potential foregrounds. As demonstrated in Fig. 2, all the anchors are represented as Gaussian distributions along the temporal dimension, Furthermore, these Gaussian temporal anchors are used

VCE to re-weight the self-attention matrices, thus enhancing the video content within the corresponding moments in the encoded video features. Specifically, given the center e^n and width v^n of n -th Gaussian temporal anchor, we generate the corresponding Gaussian distribution $G^n = \{p_i^n\}_{i=1}^{l_V}$. The density of i -th video feature p_i^n can be represented as:

$$p_i^n = \frac{1}{\sqrt{2\pi} (v^n/\gamma)} \exp\left(-\frac{(i/l_V - e^n)^2}{2 (v^n/\gamma)^2}\right), \quad (3)$$

where the γ is a scaling hyperparameter. Note that $n \in \{1, 2, \dots, N\}$, $v^n = v_{\max} \times n/N$, where N and v_{\max} are total number and the max width of anchors for each point.

By generating adequate Gaussian temporal anchors with different centers and widths, we further employ the VCE to learn the encoded video representation of each corresponding proposal. We also adopt the stacked multiple transformer encoders as the fundamental architecture for the VCE and pad a $\langle CLS \rangle$ token at the end of video feature sequences, which can be similarly represented as $F'_v = \{f'_v, f'_v^{\text{cls}}\}_{i=1}^{l_V}$. However, the multi-head self-attention weight matrices in each encoder layer will be re-weighted by different Gaussian temporal anchors. Let Φ_v be the video transformer encoders, the procedure is formulated as follows:

$$H_{v_n}^{l+1} = \Phi_v \left(f_v \left(H_{v_n}^l, G^n \right), H_{v_n}^1 = F'_v, \quad (4)$$

where $H_{v_n}^l \in \mathbb{R}^{(l_V+1) \times d_h}$ is encoded video feature sequence of n -th anchor at l -th encoder layer. $f_v(\cdot)$ is the linear projection layer. Note that the i -th row in multi-head self-attention weight matrices in multi-head self-attention of each encoder layer will be re-weighted by G^n through element-wise product.

Concept Generating. We decompose the global representations into multiple concepts for two modalities respectively, where each concept is correlated to a partial semantics and different from others. Specifically, given the final encoded global representation of a video proposal h_v^{cls} and text query h_q^{cls} , we employ two MLPs to project them into high dimensional space and conduct concept decomposing in a multi-head manner. Let $\text{Spl}(\cdot)$ be the dimension split function, this procedure can be formulated as follows:

$$C_v = \text{Spl} \left(\text{MLP}_v \left(h_v^{\text{cls}} \right), l_C \right), C_q = \text{Spl} \left(\text{MLP}_q \left(h_q^{\text{cls}} \right), l_C \right), \quad (5)$$

where $C_v, C_q \in \mathbb{R}^{l_C \times d_h}$ are text and video concepts respectively. l_C is the total number of concepts. Moreover, we also adopt the diversity loss [17] that encourages concept vectors to attend to different semantics:

$$\mathcal{L}_{\text{conc}} = \left\| C_v C_v^T - \mathbf{I} \right\|_F^2 + \left\| C_q C_q^T - \mathbf{I} \right\|_F^2, \quad (6)$$

where the $\|\cdot\|$ and \mathbf{I} represent Frobenius norm of a matrix and the identity matrix.

3.4 Semantic Reconstructor

Concept-based Language Reconstruction. Inspired by the wide success of self-supervised learning in pre-training models [2, 7], we adopt the Masked Language Modeling (MLM) to learn the deep semantics from the text queries. We randomly mask a part of keywords in the text queries, such as verbs or nouns, and require the SR module to reconstruct each masked word with the given prefix

of sentence queries and the generated concepts of two modalities. Specifically, let Ψ represents stacked multiple transformer decoders, we formulate this procedure as follows:

$$P_v = \sigma \left(f_r \left(\Psi \left(C_v, \hat{F}_q \right) \right) \right), P_q = \sigma \left(f_r \left(\Psi \left(C_q, \hat{F}_q \right) \right) \right), \quad (7)$$

where $\sigma(\cdot)$ and $f_r(\cdot)$ represent the softmax function and linear project layer respectively. \hat{F}_q are masked word-level features, where the masked words are replaced with a particular padding token. P_v and P_q are the predicted probability of each word reconstructed with video and text concepts, $P_v, P_q \in \mathbb{R}^{(l_Q \times l_W)}$. l_W is the length of word dictionary. Moreover, we adopt the log-likelihood loss to estimate the semantic reconstruction:

$$\mathcal{L}_{\text{rec}} = - \sum_{j=1}^{l_Q} \sum_{i=1}^{l_W} \hat{P} \left(\log P_v + \log P_q \right), \quad (8)$$

where \hat{P} is one-hot vector of the corresponding ground truth. The anchor with the smallest reconstruction loss is regarded as the optimal proposal, which is used to calculate the reconstruction loss of video modality.

Point-guided Contrastive Learning (PCL). Inspired by [38, 39], we conduct contrastive learning within a group of proposals within the same video to fully utilize the point-level supervision. Concretely, we apply the point-level supervision to generate multiple positive proposals. We assume that the target event moments are around the annotated points and the points are expected to be the highest density in Gaussian temporal anchors. Following the assumption, we generate multiple point-guided anchors during training while the rest parts are sampled as negative anchors, which is depicted in Fig. 2. Specifically, given three reconstruct loss of the video modality, $\mathcal{L}_{\text{rec}}^O$, $\mathcal{L}_{\text{rec}}^N$, and $\mathcal{L}_{\text{rec}}^R$, which are generated by the optimal anchor, negative anchors, and the complete video, the PCL procedure can be formulated as:

$$\mathcal{L}_{\text{pcl}} = \text{Max} \left(\mathcal{L}_{\text{rec}}^O - \mathcal{L}_{\text{rec}}^N + \alpha_1, 0 \right) + \text{Max} \left(\mathcal{L}_{\text{rec}}^O - \mathcal{L}_{\text{rec}}^R + \alpha_2, 0 \right), \quad (9)$$

where α_1 and α_2 are hyperparameters. Note that α_1 is expected to higher than α_2 as the complete video contains relevant content which is not existed in negative anchors.

Concept-based Multimodal Alignment (CMA). As one of our goals is to give up the clumsy cross-modal interactions, we align the text query with potential video proposals from the perspectives of concepts. To this end, we project the concepts of video proposals and their corresponding text queries into a common space, pushing the potential matching pairs closer while the negative pairs further. Concretely, similar to PCL module in our model, we regard the optimal anchor and the query as a matching pair while the other as negative pairs, which can be formulated as follows:

$$\begin{aligned} \mathcal{L}_{\text{cma}} = & \text{Max} \left(\text{SIM}(C_v^N, C_q) - \text{SIM}(C_v^O, C_q) + \alpha_3, 0 \right) + \\ & \text{Max} \left(\text{SIM}(C_v^R, C_q) - \text{SIM}(C_v^O, C_q) + \alpha_4, 0 \right) + \\ & \text{MSE} \left(C_v^O, C_q \right), \end{aligned} \quad (10)$$

where C_v^O , C_v^N , and C_v^R represent the video concepts generated by the optimal video anchor, negative anchors, and the complete

video respectively. C_q is the text concept of the corresponding query. $\text{SIM}(\cdot)$ and $\text{MSE}(\cdot)$ are the cosine similarity calculation and Mean Squared Error loss. α_3 and α_4 are hyperparameters, similarly, $\alpha_3 \leq \alpha_4$.

3.5 Training and Inference

We employ multi-scale strategies in generating Gaussian temporal anchors. As illustrated in Fig. 2, we take single scale of anchor width as an example here for explicit. During training, we regard the point-level supervision as center to generate a positive Gaussian temporal anchors during training. The rest of video parts are regarded as two negative anchors. Let β_1 and β_2 be balance factors, the overall training objective can be represented as follows:

$$\mathcal{L}_{\text{total}} = \mathcal{L}_{\text{conc}} + \mathcal{L}_{\text{cma}} + \beta_1 \mathcal{L}_{\text{rec}} + \beta_2 \mathcal{L}_{\text{pcl}}. \quad (11)$$

During inference, we sample time points along the temporal dimension evenly as the center of Gaussian temporal anchors. Moreover, the SR module is disabled and the VCE module can be simply integrated into the video feature extractors, turning untrimmed videos into a group of concepts *in an offline manner*. Hence, the online cross-modal interactions are not required. We only need to deploy the TCE to learn the text concepts and calculate cosine similarity with the concepts of multiple Gaussian temporal anchors. As a result, the computational cost during inference can be significantly reduced in our CFMR method.

4 EXPERIMENTS

4.1 Experimental Settings

Datasets. As we aim to tackle the PS-VMR task, where the temporal annotations are not available during training but only the rough point-level annotations, we adopt the same point-level annotations with [6] for fairness. The general information of adopted three datasets is summarized as follows: **(1) Charades-STA** [9]: It contains 6,672 daily life videos in averaged 29.76 seconds and involves 16,128 video-query pairs. In general, the dataset is split into training and testing parts with 12408 pairs and 3720 pairs, respectively. **(2) TACoS** [29]: It consists of 127 long videos in averaged 287.14 seconds which contain different activities that happened in the kitchen room. A standard split [9] consists of 10146, 4589, and 4083 video-sentence pairs for training, validation, and testing, respectively. **(3) ActivityNet-Captions** [14]: It contains around 20k open domain videos in averaged 117.61 seconds for video grounding tasks. It is split into the training, val, and test of 37421, 17505, and 17031 cases respectively.

Implementation Details. Following the previous methods [6, 37, 39], we adopt the pre-trained I3D [4] backbone for the Charades-STA dataset and the C3D [31] backbone for the ActivityNet-Captions and TACoS datasets. Furthermore, we evenly sample the max lengths of video features l_v into 200, 200, and 512 while number of concept is set to 7, 8, 3 for the Charades-STA, ActivityNet-Captions, and TACoS datasets respectively. The max length of the text query l_Q is set to 20. As for the Gaussian temporal anchors, we set the hyperparameter γ to 9. The max temporal lengths are set to 0.8, 0.6, 0.3, while the number of center points during inference is set to 8, 4, 15 for the three datasets respectively. v_{max} is set to 0.55, 0.66, and 0.3 respectively, while N is set to 3. We train the CFMR on a single

Nvidia RTX 3090 with 32 batchsize. The Adam optimizer [13] is employed to update the parameters with the learning rate set to 4×10^{-4} . *For more implementation details, please kindly refer to our supplementary materials and implementation codes.*

Evaluation Metrics. Following the previous methods [6, 37, 39], we adopt the recall rate as performance metrics, which is denoted as $\text{Recall}@TopK, IoU = m$ and abbreviated as $R@K, IoU = m$, where K is the top range number of ranked generated candidates and m is the threshold. Specifically, for the three datasets, k is all set to 5, while m is set to $\{0.5, 0.7\}$, $\{0.5, 0.7\}$, and $\{0.3, 0.5\}$ for Charades-STA, ActivityNet-Captions, and TACoS respectively. Considering the test time can be influenced by hardwares, we evaluate the floating-point operations per second (FLOPs) and parameters to show the model efficiency.

4.2 Overall Comparison Results

We compare the performance and efficiency with recent state-of-the-art VMR methods, including: **(1) FS-VMR methods:** 2DTAN [37], LGI [25], SS [8], FVMR [10], and CDN [33]. **(2) WS-VMR methods:** SCN [18], CWG [5], CNM [38], and CPL [39]. **(3) PS-VMR methods:** P-LGI [25], P-SCN [18], P-CPL [39], ViGA [6], and PSVTG [35]. As the PS-VMR methods are not fully explored yet, we extend [18, 25, 39] to P-LGI, P-SCN, and P-CPL respectively by introducing the point-level supervision with L_1 loss.

Table 1: Accuracy compared with the state-of-the-arts on the Charades-STA dataset using I3D features.

Type	Method	R@1, IoU=0.5	R@1, IoU=0.7	R@5, IoU=0.5	R@5, IoU=0.7
FS	2DTAN [37]	50.62	28.71	79.92	48.52
	LGI [25]	59.46	35.48	-	-
	SS [8]	56.97	32.74	88.65	56.91
	FVMR [10]	55.01	33.74	89.17	57.24
	CDN [33]	51.75	29.45	78.47	54.76
WS	SCN [18]	23.58	9.97	71.80	38.87
	CNM [38]	35.43	15.45	-	-
	CWG [5]	31.02	16.53	77.53	41.91
	CPL [39]	49.24	22.39	84.71	52.37
PS	P-LGI [25]	25.67	7.98	-	-
	P-SCN [18]	21.73	5.52	58.57	24.97
	P-CPL [39]	50.27	<u>22.16</u>	84.97	<u>52.41</u>
	ViGA [6]	45.05	20.27	59.87	35.24
	PSVTG [35]	39.22	20.17	-	-
	CFMR (Ours)	<u>48.14</u>	22.58	<u>80.06</u>	56.09

Comparisons on Accuracy. We compare the performance of our proposed CFMR method with recent state-of-the-art methods using the same video feature extractors. The results on the three benchmarks are reported in Table 1, 2, and 3 respectively, where the best performance and the suboptimal performance are bold and underlined respectively.

Based on the experimental results, we list the following observations: (1) Our proposed CFMR method significantly outperforms the recent state-of-the-art PS-VMR methods on most metrics. Specifically, it gains at almost 20% improvement on the metrics of Recall@5

Table 2: Accuracy compared with the state-of-the-arts on the TACoS dataset using C3D features.

Type	Method	R@1, IoU=0.3	R@1, IoU=0.5	R@5, IoU=0.3	R@5, IoU=0.5
FS	2DTAN [37]	37.29	25.32	57.81	45.04
	SS [8]	41.33	29.56	60.65	48.01
	FVMR [10]	41.48	29.12	64.53	50.00
	CDN [33]	43.09	32.82	64.98	52.96
WS	SCN [18]	11.72	4.75	23.82	11.22
	CNM [38]	7.20	2.20	-	-
	CPL [39]	11.42	4.12	33.37	15.00
PS	P-SCN [18]	11.50	3.50	24.34	10.17
	P-CPL [39]	13.77	4.97	<u>34.67</u>	<u>15.97</u>
	ViGA [6]	19.62	8.85	26.17	14.20
	PSVTG [35]	<u>23.64</u>	<u>10.00</u>	-	-
	CFMR (Ours)	25.44	12.82	49.01	28.52

Table 3: Accuracy compared with the state-of-the-arts on the ActivityNet-Captions dataset using C3D features.

Type	Method	R@1, IoU=0.5	R@1, IoU=0.7	R@5, IoU=0.5	R@5, IoU=0.7
FS	2DTAN [37]	44.51	26.54	77.13	61.96
	LGI [25]	41.51	23.07	-	-
	SS [8]	46.67	27.56	78.37	63.78
	FVMR [10]	45.00	26.85	77.42	61.04
WS	SCN [18]	29.22	-	55.69	-
	CNM [38]	30.26	12.81	-	-
	CWG [5]	29.52	-	66.61	-
	CPL [39]	31.67	13.53	43.23	22.14
PS	P-LGI [25]	4.11	1.31	-	-
	P-SCN [18]	21.91	12.60	49.54	21.91
	P-CPL [39]	31.10	12.79	35.37	16.61
	ViGA [6]	<u>35.79</u>	16.96	<u>53.12</u>	<u>33.01</u>
	PSVTG [35]	35.59	21.98	-	-
	CFMR (Ours)	36.97	<u>17.33</u>	69.28	49.40

compared with the initial PS-VMR method, *i.e.*, ViGA [6]. Compared with the latest PS-VMR method that supports retrieving the single moment only, *i.e.*, PSVTG, the CFMR method with multiple candidates still makes remarkable progress on most metrics and is more practical in retrieval systems. It proves the superiority of the proposed CFMR method, which effectively mines hidden semantics with point-level supervision and learns concept-based multimodal alignments only. (2) By introducing curriculum learning to explore potential target moment, the latest WS-VMR method, CPL [39] and the extended version P-CPL, achieve better performance on Charades-STA dataset on a few low-precision metrics. However, they show obvious weaknesses in the other two datasets that mainly consist of long untrimmed videos. A probable is long untrimmed videos contain more irrelevant content and are more challenging for model robustness. It also proves that arbitrarily giving up all temporal supervision to reduce the annotation cost is unreasonable and harmful to the generalization of VMR. (3) We also note that our method is suboptimal on the R1@IoU=0.7 than the optimal PSTVG

method [35] on the ActivityNet-Captions dataset. We speculate the reason is there exists a number of recapitulative query cases in this dataset, which are related to the whole video. As the proposed CFMR turns the whole video into Gaussian temporal anchors, it is hard to retrieve the complete videos with recapitulative queries.

Comparisons on Efficiency. To evaluate the comprehensive performance, we count the FLOPs and Parameters of counterpart methods [6, 18, 25, 33, 37–39] based on their official open-source implementation codes. Note that the previous FS-VMR method, *i.e.*, FVMR [10], employs knowledge distillation to improve model efficiency. Considering the experimental results are measured by test time and the implementation codes are inaccessible, it can hardly make fair comparisons here. In theory, we speculate the FVMR should have similar efficiency to ours as the cross-modal interactions can be bypassed in the test stage through knowledge transfer. However, the knowledge distillation in FVMR is *highly reliant on fully annotated data*, which still requires massive annotation cost and can not be introduced into the WS-VMR or PS-VMR paradigms.

According to the comparisons listed in Tabel 4, we list following observations: (1) Our proposed CFMR method is superior to the other methods on efficiency. Specifically, compared the previous state-of-the-art PS-VMR method [6], our method saves more than $100 \times$ FLOPs with 20% parameters. The reason is our method extracts the video concepts during offline visual feature extraction and models the text query online only. Bypasses the complicated cross-modal interactions, it requires much less computational cost. (2) The efficiency of our method is less sensitive to video data. This is because massive calculation in previous VMR methods can not be propelled until receiving text queries. Contrastively, the proposed CFMR process video data in an offline manner thus requires no extra calculation in retrieval but text encoding. (3) With higher efficiency, our method still achieves competitive performance on retrieving event moment. Our method gets at least 16% improvements on the Acc@5 than other PS-VMR methods while also reaching the top-rank performance on the Acc@1. It explicates that our method effectively maintains retrieval accuracy while significantly reducing computational resources and annotation cost.

4.3 Further Analysis

Analysis on Training Objectives. To furtherly explore the effectiveness of each component in our method, we conduct the ablation study on training objectives. From the experimental results listed in Table 5, we can observe that: (1) By introducing the \mathcal{L}_{rec} , the proposed CFMR obtains remarkable improvements. It demonstrate the SR module is crucial for learning hidden semantics to generate correct concepts for the two modalities. (2) The ablated model obtains significantly improvement with \mathcal{L}_{pcl} . The reason is our CFMR method relies on the PCL module to learn semantic cues of matched text and video pairs. (3) The CMA module performs an important role in our CFMR method. By applying \mathcal{L}_{cma} , the ablated model achieves great improvements on both two datasets. This is because we give up retrieving video moments with cross-modal interactions but aligning the two modality at concept-level. Hence, the CMA module is essential for guiding the two encoders to learn common concepts of related video proposals and text queries. (4) We can also observe that both \mathcal{L}_{rec} and \mathcal{L}_{pcl} improve the model

Table 4: Overall comparisons on FLOPs ($\times 10^8$), Parameters ($\times 10^6$), and Accuracy. Considering the length of videos, we select IoU as 0.7, 0.5, 0.3 to evaluate the accuracy for Charades-STA, ActivityNet-Captions, and TACoS respectively. All the results are estimated by averaging the same test cases. For fairness, we ignore offline calculations in compared methods.

Type	Method	Charades-STA				ActivityNet-Captions				TACoS			
		FLOPs ↓	Params ↓	Acc@1 ↑	Acc@5 ↑	FLOPs ↓	Params ↓	Acc@1 ↑	Acc@5 ↑	FLOPs ↓	Params ↓	Acc@1 ↑	Acc@5 ↑
FS	2D-TAN	515.90	52.43	28.71	48.52	4973.81	84.94	44.51	77.13	10615.91	52.43	37.29	57.81
	LGI	34.65	29.12	35.48	-	56.94	47.21	41.64	-	-	-	-	-
	CDN	136.37	238.14	29.45	54.76	-	-	-	-	8594.02	238.14	43.09	64.98
WS	SCN	8.25	5.38	9.97	38.87	11.01	7.01	29.22	55.69	19.35	6.46	11.72	23.82
	CNM	5.38	5.37	15.45	-	5.33	7.01	28.70	-	15.02	6.46	7.20	-
	CPL	37.52	5.38	22.39	52.37	51.65	7.01	31.76	43.23	98.16	6.46	11.42	33.37
PS	P-SCN	8.25	5.38	5.52	24.57	11.01	7.01	21.91	49.54	19.35	6.46	11.50	24.34
	ViGA	16.82	12.61	19.09	32.82	17.81	12.61	35.79	53.12	38.45	12.61	19.67	26.17
	CFMR (Ours)	0.16	2.98	22.58	56.09	0.22	3.04	36.97	69.28	0.19	2.71	25.44	49.01

Table 5: Ablation study on the Charades-STA dataset.

$\mathcal{L}_{\text{conc}}$	\mathcal{L}_{rec}	\mathcal{L}_{pcl}	\mathcal{L}_{cma}	R@1, IoU=0.5	R@1, IoU=0.7	R@5, IoU=0.5	R@5, IoU=0.7
✓	✗	✗	✗	10.94	3.74	41.81	22.49
✓	✓	✗	✗	23.44	8.03	55.39	32.27
✓	✓	✓	✗	30.09	11.93	63.79	39.92
✗	✗	✗	✓	32.89	13.15	69.50	46.01
✗	✗	✓	✓	35.38	15.41	71.96	43.53
✗	✓	✗	✓	38.17	16.00	75.24	51.16
✗	✓	✓	✓	47.31	21.35	79.63	54.34
✓	✓	✓	✓	48.14	22.58	80.06	56.09

performance. However, the combination of the three loss functions, *i.e.*, $\mathcal{L}_{\text{cma}} + \mathcal{L}_{\text{rec}} + \mathcal{L}_{\text{pcl}}$, significantly boosts the retrieval performance. The reason is $\mathcal{L}_{\text{rec}} + \mathcal{L}_{\text{pcl}}$ can guide our model to learn which video anchor matches the text query best. Hence, the CMA process is more effective since the reliability of selected positive video concepts improved.

Table 6: Analysis with respect to concept number l_c on the Charades-STA dataset with I3D features.

Concept Number	R@1, IoU=0.5	R@1, IoU=0.7	R@5, IoU=0.5	R@5, IoU=0.7	MFLOPs	Params
4	46.47	20.96	79.58	55.20	15.74	2.78
5	47.09	21.42	81.06	56.44	15.81	2.85
6	47.36	22.52	80.06	56.41	15.87	2.91
7	48.14	22.58	80.06	56.09	15.94	2.98
8	47.58	21.85	78.85	55.79	16.01	3.04

Analysis on Concept-based Multimodal Alignments. We also take a closer look at the CMA module procedure to explore how the generated concepts influence the comprehensive performance of the whole model. Specifically, we conduct further analysis on the number of concepts l_c and visualize generated concepts of two modalities via t-SNE [32]. By observing Table 6 and Fig. 3, we can see: (1) More concepts will not increase the performance as expected. With the number of concept increasing, the recall rate increases slowly but stops at $l_c = 7$. It explicates that information granularity has impacts on learning the semantics in two modalities. Hence, an appropriate setting is critical in estimating the semantic

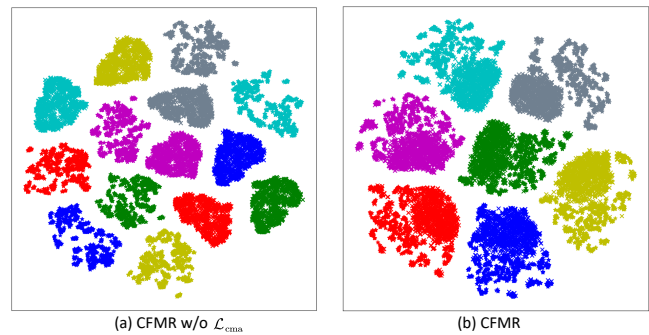


Figure 3: Visualization of multimodal concepts with t-SNE. The colors and shapes represent the numbers and types of modalities respectively, where “★” is text concept and “×” is video concept.

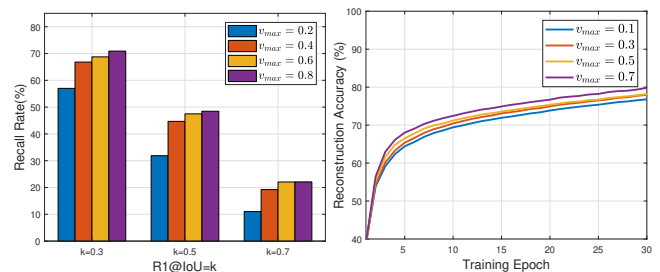


Figure 4: Analysis on performance of moment retrieval and language reconstruction with different v_{max} in PCL module.

similarity. (2) The computational consumption increases linearly with more concepts but is still superior to the other methods. This is because our CFMR methods tackle the VMR task without heavy cross-modal interactions in the inference stage, which means the video can be processed in an offline manner with visual extractors. (3) By applying \mathcal{L}_{cma} , the concepts show a clustering tendency and the concepts of video proposals are hybrid with the concepts of corresponding text queries. It demonstrates that the CMA module in our method effectively learns diverse semantics and generates similar concepts for related video proposals and text queries.

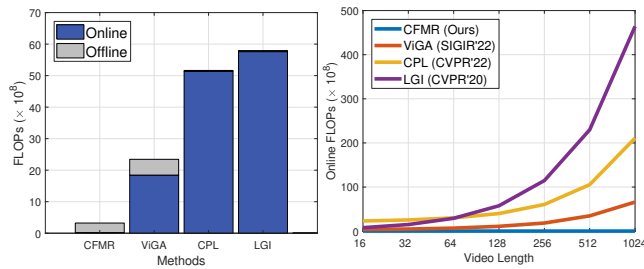


Figure 5: Comparisons w.r.t online and offline FLOPs on the ActivityNet-Captions dataset.

Analysis on Point-guided Contrastive Learning. We also further explore the procedure of SR module in our CFMR model. Concretely, we conduct experiments with different settings on the max widths v_{\max} and observe corresponding performance of moment retrieval as well as the language reconstruction. According to the results in Fig. 4, we list following observations: (1) The reconstruction accuracy shows positive correlations to the performance of moment retrieval. We can see that the ablated models with higher VMR recall rates obtain more high-quality semantic reconstruction. It proves again the SR module is effective to learn the hidden semantics in video and text modalities, which helps generate relevant common concepts. (2) It is helpful to increase the scales of the temporal receptive field in PCL. By introducing larger max widths of positive anchors v_{\max} , the CFMR achieves remarkable improvements in the performance of retrieval and language reconstruction both. However, we also note that such a strategy is limited as the improvements become less significant at $v_{\max} = 0.8$. The reason is oversized temporal receptive fields bring massive irrelevant content, which leads to degeneration in the contrastive learning among positive and negative samples.

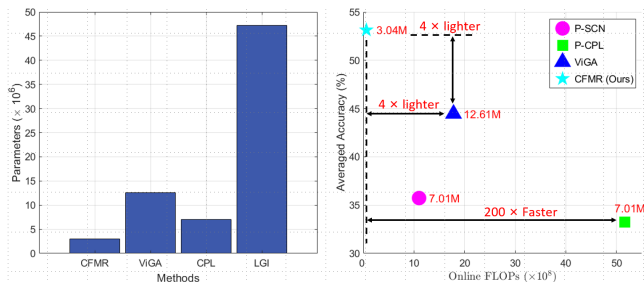


Figure 6: Analysis with respect to model parameters and comprehensive performance, including averaged accuracy ($R1@IoU=0.5$ and $R5@IoU=0.5$), model parameters ($\times 10^6$), and FLOPs $\times 10^8$ on the ActivityNet-Captions dataset.

Analysis on Efficiency. We also show more details of computational consumption in the CFMR method and make a comparison with other VMR methods [6, 25, 39]. Specifically, We count the offline (processing one video) and online (processing one query and cross-modal interactions) FLOPs to furtherly demonstrate the superiority of our model. According to the comparative results in Fig. 5, we obtain following observations: (1) The CFMR significantly

reduces the proportion of online computational cost. Facilitated with concept-based retrieval rather than cross-modal interactions, it requires no extra online computation but only encoding users’ text queries online. (2) With the untrimmed videos get longer, our method keeps high efficiency while the computational consumption of others increase dramatically. It demonstrates the previous methods heavily suffer from the complex online cross-modal interactions which are sensitive to videos. Contrastively, our CFMR effectively tackles this problem by eliminating this inflexible design to maintain remarkable performance.

To furtherly show the superiority of the model efficiency, we also count parameters of the CFMR method and make comparisons with the other methods. As is illustrated in Fig. 6, our method is much lighter, which only requires less than one quarter of parameters of the previous PS-VMR ViGA method. Moreover, we comprehensively compare our CFMR method to several PS-VMR methods in Fig. 6 by observing their online FLOPs, parameters, and accuracy. It can be seen our CFMR achieve remarkable improvement on the averaged moment retrieval accuracy, while is $80 \times$ faster and $4 \times$ lighter than the existing state-of-the-art ViGA method.

Table 7: Comparisons on model performance on the ActivityNet-CD-OOD debiased datasets with C3D features.

Method	R@1, IoU=0.5	R@1, IoU=0.7	R@5, IoU=0.5	R@5, IoU=0.7
CNM [38]	7.13	0.43	-	-
CPL [39]	8.71	1.63	14.24	3.24
P-CPL [39]	9.21	1.33	11.44	2.21
ViGA [6]	20.28	8.12	30.21	16.13
CFMR (Ours)	21.59	9.76	49.43	32.24

Performance on Out-Of-Distribution Settings. Furthermore, we also conduct more experiments under the out-of-distribution (OOD) settings to evaluate the robustness and generalizing strength of our CFMR method. Specifically, we adopt the data split proposed in [36], where the ground-truth moment distribution is different in the training and test splits. Similarly, only point-level annotations are provided in the training split to reduce the training data cost. We report the experimental results on the ActivityNet-CD-OOD datasets in Table 7 and compared with recent FS-VMR, WS-VMR, and PS-VMR methods. It can be observe that our method still achieves remarkable improvements compared with the counterpart ViGA method [6], especially on the metrics of R@5. This is because our method deploys the CMA module and PCL module, which effectively extract hidden semantics and conduct concept-based multimodal alignments with point-level supervision signals.

Qualitative Analysis. We also illustrate the qualitative analysis in Fig. 7 obtained by our CFMR method and the latest counterpart ViGA method [6]. According to the visualization results, our CFMR reveals remarkable superiority in retrieval accuracy and also achieves higher retrieval efficiency over the ViGA method. Specifically, it takes only 3 milliseconds nearly to retrieve the most correlated moment precisely for our CFMR method, while more than 40 milliseconds for the previous ViGA method. Such a result

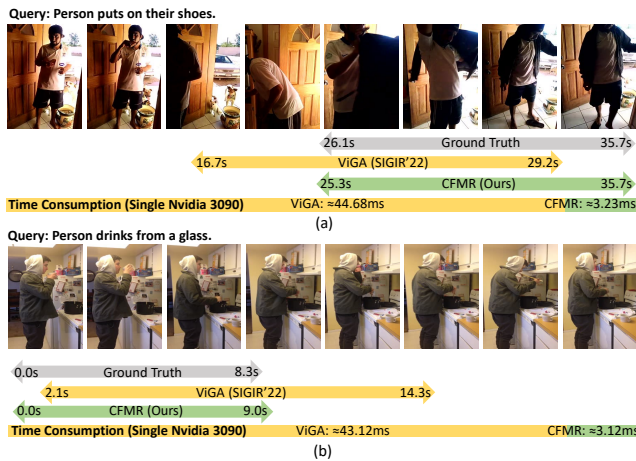


Figure 7: Visualization of two examples of moment retrieval results and time consumption on the Charades-STA dataset.

explicates again the effectiveness of our proposed CFMR method, which eliminates the cross-modal interactions in the test stage and fast aligns two modalities with diverse semantic concepts to retrieve the target moment.

5 CONCLUSION

In this paper, we proposed a Cheaper and Faster Moment Retrieval (CFMR) method to achieve a fair trade-off among retrieval accuracy, efficiency, and annotation cost for the VMR task. It can be trained with much cheaper point-level supervision but shows competitive retrieval performance. Moreover, unlike existing methods, our CFMR method bypasses the cross-modal interaction modules in previous VMR methods thus greatly optimizing model efficiency. Extensive experiments on three widely adopted benchmarks demonstrated the remarkable performance of the proposed CFMR method. For future work, we will explore more practical VMR methods to furtherly facilitate the development of relevant applications.

REFERENCES

- [1] Lisa Anne Hendricks, Oliver Wang, Eli Shechtman, Josef Sivic, Trevor Darrell, and Bryan Russell. 2017. Localizing moments in video with natural language. In *IEEE International Conference on Computer Vision*. 5803–5812.
- [2] Hangbo Bao, Li Dong, and Furu Wei. 2021. Beit: Bert pre-training of image transformers. *arXiv preprint arXiv:2106.08254* (2021).
- [3] Amy Bearman, Olga Russakovsky, Vittorio Ferrari, and Li Fei-Fei. 2016. What’s the point: Semantic segmentation with point supervision. In *European Conference on Computer Vision*. 549–565.
- [4] João Carreira and Andrew Zisserman. 2017. Quo Vadis, Action Recognition? A New Model and the Kinetics Dataset. In *IEEE Conference on Computer Vision and Pattern Recognition*. 4724–4733.
- [5] Jiaming Chen, Weixin Luo, Wei Zhang, and Lin Ma. 2022. Explore Inter-contrast between Videos via Composition for Weakly Supervised Temporal Sentence Grounding. In *AAAI Conference on Artificial Intelligence*. 267–275.
- [6] Ran Cui, Tianwen Qian, Pai Peng, Elena Daskalaki, Jingjing Chen, Xiaowei Guo, Huiyuan Sun, and Yu-Gang Jiang. 2022. Video Moment Retrieval from Text Queries via Single Frame Annotation. In *International ACM SIGIR Conference on Research & Development in Information Retrieval*. 1033–1043.
- [7] Jacob Devlin, Ming-Wei Chang, Kenton Lee, and Kristina Toutanova. 2019. BERT: Pre-training of Deep Bidirectional Transformers for Language Understanding. In *Conference of the North American Chapter of the Association for Computational Linguistics: Human Language Technologies*. 4171–4186.
- [8] Xinpeng Ding, Nannan Wang, Shiwei Zhang, De Cheng, Xiaomeng Li, Ziyuan Huang, Mingqian Tang, and Xinbo Gao. 2021. Support-set based cross-supervision for video grounding. In *IEEE International Conference on Computer Vision*. 11573–11582.
- [9] Jiyang Gao, Chen Sun, Zhenheng Yang, and Ram Nevatia. 2017. Tall: Temporal activity localization via language query. In *IEEE International Conference on Computer Vision*. 5267–5275.
- [10] Junyu Gao and Changsheng Xu. 2021. Fast video moment retrieval. In *IEEE International Conference on Computer Vision*. 1523–1532.
- [11] Junyu Gao and Changsheng Xu. 2021. Learning video moment retrieval without a single annotated video. *IEEE Transactions on Circuits and Systems for Video Technology* 32, 3 (2021), 1646–1657.
- [12] Xun Jiang, Xing Xu, Jingran Zhang, Fumin Shen, Zuo Cao, and Heng Tao Shen. 2022. Semi-Supervised Video Paragraph Grounding With Contrastive Encoder. In *IEEE Conference on Computer Vision and Pattern Recognition*. 2466–2475.
- [13] Diederik P. Kingma and Jimmy Ba. 2015. Adam: A Method for Stochastic Optimization. In *International Conference on Learning Representations*.
- [14] Ranjay Krishna, Kenji Hata, Frederic Ren, Li Fei-Fei, and Juan Carlos Niebles. 2017. Dense-Captioning Events in Videos. In *IEEE International Conference on Computer Vision*. 706–715.
- [15] Issam H Laradji, Negar Rostamzadeh, Pedro O Pinheiro, David Vazquez, and Mark Schmidt. 2018. Where are the blobs: Counting by localization with point supervision. In *European Conference on Computer Vision*. 547–562.
- [16] Pilhyeon Lee and Hyeran Byun. 2021. Learning action completeness from points for weakly-supervised temporal action localization. In *IEEE International Conference on Computer Vision*. 13648–13657.
- [17] Zhouhan Lin, Minwei Feng, Cicero Nogueira dos Santos, Mo Yu, Bing Xiang, Bowen Zhou, and Yoshua Bengio. 2017. A structured self-attentive sentence embedding. *arXiv preprint arXiv:1703.03130* (2017).
- [18] Zhijie Lin, Zhou Zhao, Zhu Zhang, Qi Wang, and Huasheng Liu. 2020. Weakly-supervised video moment retrieval via semantic completion network. In *AAAI Conference on Artificial Intelligence*. 11539–11546.
- [19] Daizong Liu, Xiaoye Qu, Yinzhen Wang, Xing Di, Kai Zou, Yu Cheng, Zichuan Xu, and Pan Zhou. 2022. Unsupervised temporal video grounding with deep semantic clustering. *arXiv preprint arXiv:2201.05307* (2022).
- [20] Fan Luo, Shaoxiang Chen, Jingjing Chen, Zuxuan Wu, and Yu-Gang Jiang. 2021. Self-supervised learning for semi-supervised temporal language grounding. *arXiv preprint arXiv:2109.11475* (2021).
- [21] Fan Ma, Linchao Zhu, Yi Yang, Shengxin Zha, Gourab Kundu, Matt Feiszli, and Zheng Shou. 2020. Sf-net: Single-frame supervision for temporal action localization. In *European conference on computer vision*. 420–437.
- [22] Pascal Mettes, Jan C van Gemert, and Cees GM Snoek. 2016. Spot on: Action localization from point-to-supervised proposals. In *European Conference on Computer Vision*. 437–453.
- [23] Niluthpol Chowdhury Mithun, Sujoy Paul, and Amit K. Roy-Chowdhury. 2019. Weakly Supervised Video Moment Retrieval From Text Queries. In *Computer Vision and Pattern Recognition*. 11592–11601.
- [24] Davide Moltisanti, Sanja Fidler, and Dima Damen. 2019. Action recognition from single timestamp supervision in untrimmed videos. In *IEEE Conference on Computer Vision and Pattern Recognition*. 9915–9924.
- [25] Jonghwan Mun, Minsu Cho, and Bohyung Han. 2020. Local-Global Video-Text Interactions for Temporal Grounding. In *IEEE Conference on Computer Vision and Pattern Recognition*. 10807–10816.
- [26] Jinwoo Nam, Daechul Ahn, Dongyeop Kang, Seong Jong Ha, and Jonghyun Choi. 2021. Zero-shot natural language video localization. In *IEEE International Conference on Computer Vision*. 1470–1479.
- [27] Jeffrey Pennington, Richard Socher, and Christopher D. Manning. 2014. Glove: Global Vectors for Word Representation. In *Conference on Empirical Methods in Natural Language Processing*. 1532–1543.
- [28] Joseph Redmon, Santosh Divvala, Ross Girshick, and Ali Farhadi. 2016. You only look once: Unified, real-time object detection. In *Proceedings of the IEEE conference on computer vision and pattern recognition*. 779–788.
- [29] Michaela Regneri, Marcus Rohrbach, Dominikus Wetzels, Stefan Thater, Bernt Schiele, and Manfred Pinkal. 2013. Grounding Action Descriptions in Videos. *Transactions of the Association for Computational Linguistics* 1 (2013), 25–36.
- [30] Shaoqing Ren, Kaiming He, Ross B. Girshick, and Jian Sun. 2017. Faster R-CNN: Towards Real-Time Object Detection with Region Proposal Networks. *IEEE Transactions on Pattern Analysis and Machine Intelligence* 39, 6 (2017), 1137–1149.
- [31] Du Tran, Lubomir Bourdev, Rob Fergus, Lorenzo Torresani, and Manohar Paluri. 2015. Learning spatiotemporal features with 3d convolutional networks. In *IEEE International Conference on Computer Vision*. 4489–4497.
- [32] Laurens Van der Maaten and Geoffrey Hinton. 2008. Visualizing data using t-SNE. *Journal of Machine Learning Research* 9, 11 (2008).
- [33] Gongmian Wang, Xing Xu, Fumin Shen, Huimin Lu, Yanli Ji, and Heng Tao Shen. 2022. Cross-modal dynamic networks for video moment retrieval with text query. *IEEE Transactions on Multimedia* 24 (2022), 1221–1232.
- [34] Yi Wang, Junhui Hou, Xinyu Hou, and Lap-Pui Chau. 2021. A self-training approach for point-supervised object detection and counting in crowds. *IEEE Transactions on Image Processing* 30 (2021), 2876–2887.

- [35] Zhe Xu, Kun Wei, Xu Yang, and Cheng Deng. 2022. Point-Supervised Video Temporal Grounding. *IEEE Transactions on Multimedia* (2022).
- [36] Yitian Yuan, Xiaohan Lan, Long Chen, Wei Liu, Xin Wang, and Wenwu Zhu. 2021. A Closer Look at Temporal Sentence Grounding in Videos: Datasets and Metrics. *arXiv preprint arXiv:2101.09028* (2021).
- [37] Songyang Zhang, Houwen Peng, Jianlong Fu, and Jiebo Luo. 2020. Learning 2D Temporal Adjacent Networks for Moment Localization with Natural Language. In *AAAI Conference on Artificial Intelligence*. 12870–12877.
- [38] Minghang Zheng, Yanjie Huang, Qingchao Chen, and Yang Liu. 2022. Weakly Supervised Video Moment Localization with Contrastive Negative Sample Mining. In *AAAI Conference on Artificial Intelligence*. 3517–3525.
- [39] Minghang Zheng, Yanjie Huang, Qingchao Chen, Yuxin Peng, and Yang Liu. 2022. Weakly Supervised Temporal Sentence Grounding With Gaussian-Based Contrastive Proposal Learning. In *IEEE Conference on Computer Vision and Pattern Recognition*. 15555–15564.